

The one-particle Green's function of one-dimensional insulating materials

M. C. Refolio, J. M. López Sancho, and J. Rubio

Instituto de Matemáticas y Física Fundamental, CSIC

Serrano 113 bis, E-28006 Madrid, Spain

J. A. Verges

Instituto de Ciencia de Materiales ICM-M-CCS, I

Cantoblanco, E-28049 Madrid, Spain

(Dated: April 14, 2024)

The single particle spectral-weight function (SWF) of the ionic Hubbard model at half filling is calculated in the cluster perturbation theory approximation. An abrupt change of regime in the low-energy region, near the chemical potential, is found at a critical value, U_c , of the coupling constant (Hubbard U). The SWF at the Fermi points $k_F = \pm 2$ jumps, as U increases, from a two-peak structure, the gap edges, to a four-peak structure accompanied by a (non-vanishing) minimum of the charge-gap. The two inner peaks of this structure show very small dispersion (flat bands) away from the Fermi points, whereas the outer peaks mark the edges of the Hubbard bands. No other signatures of abrupt change are detected in the SWF. The two regimes are physically realized in the angle-resolved photoelectron spectra of $(\text{TaSe}_4)_2\text{I}$, and the blue-bronze $\text{K}_{0.3}\text{MnO}_3$, respectively.

PACS numbers: 71.10.-w, 71.10.Fd, 71.10.Hf, 71.30.+h

I. INTRODUCTION

Quasi-one-dimensional (Q1D) systems have been the object of intense experimental and theoretical activity over the last twenty years. They show highly anisotropic properties, with a privileged direction of enhanced charge transport. Their interest lies in the hope that they can be good candidates for the physical realization of non-Fermi liquid behavior. This interest, in low-D systems in general, has expanded very rapidly in recent years partly due

to the technological development of low-D artificial structures and nano-scale materials.

Above their Peirls temperature (or when doped away from half filling), these Q1D systems are conductors and display Luttinger liquid behavior¹, i.e., the absence of quasi-particle excitations in the Fermi liquid sense (a quasi-particle peak at the Fermi level) and the excitation, instead, of decoupled collective modes of charge (holons) and spin (spinons) character, a phenomenon usually known as charge-spin separation. The absence of a Fermi edge has indeed been found in angle-resolved photoelectron spectroscopy (ARPES) of $(\text{TaSe}_4)_2\text{I}^{2,3}$, $\text{K}_{0.3}\text{MnO}_3$ ⁴, and the organic conductor TTF-TCNQ (tetrathiafulvalene-tetracyanoquinodimethane)^{5,6}. For a good review, see Ref 7. Clear experimental signatures of spin-charge separation are, however, very scarce in Q1D conductors, with the notable exception of TTF-TCNQ reported very recently⁶. All these compounds in their metallic state can be modeled by the low-energy physics of the doped 1D single-band Hubbard Hamiltonian⁶. Alternatively, they have been analyzed on the basis of the Luttinger model or the Luther-Emery model (when a spin gap is expected). Some puzzles still remain unsolved⁷.

Below their Peirls temperature, these Q1D compounds, as well as many others like halogen-bridged transition-metal chains, conjugated polymers, and organic charge-transfer salts are usually insulating. In these systems, the competition between strong on-site correlations and their kinetic energy gives rise to significant localization of their itinerant electrons. This often leads to the stabilization of non-metallic ground states with or without charge-density waves (CDW). Thus $(\text{TaSe}_4)_2\text{I}$ and the blue bronze $\text{K}_{0.3}\text{MnO}_3$, for instance, are CDW insulators⁷, while the nearly ideal 1D CuO chains in SrCuO_2 and Sr_2CuO_3 are responsible for the insulating character of these charge-transfer insulators⁸. Signatures of spin-charge separation have also been found in ARPES of SrCuO_2 ⁹ and in the dielectric response of Sr_2CuO_3 ¹⁰.

Most of these insulating systems can be conveniently described by the Emery model¹¹, which is a generalized Hubbard Hamiltonian on a two-sublattice model, made of cations (say Cu ions) and anions (say O ions), respectively. The on-site energy levels and repulsions (ϵ_d, U_{dd}) and (ϵ_p, U_{pp}), for Cu d orbitals and O p orbitals, are coupled by nearest-neighbor hopping of strength t_{dp} and Coulomb repulsions V_{dp} . Its 1D version reads

$$H = \sum_{is} \epsilon_d n_{dis} + U_{dd} \sum_i n_{di} n_{di\#} + \sum_{js} \epsilon_p n_{pjs} + U_{pp} \sum_j n_{pj} n_{pj\#} \quad (1)$$

$$+ t_{dp} \sum_{\langle ij \rangle s} (d_{is}^{\dagger} p_{js} + hc) + V_{dp} \sum_{\langle ij \rangle} n_{di} n_{pj}$$

where d_{is}^{\dagger} creates an electron (hole) in a d orbital at site i with spin s , i running over all the Cu sites. Similarly p_{js} annihilates an electron (hole) in a p orbital at site j and spin s , j running over all the O sites. As usual, $\langle ij \rangle$ means summation over nearest-neighbors, $n_s = c_s^{\dagger} c_s$ and $n_i = n_{i\#} + n_{i\#}$ denotes the charge at the i th site.

We may now simplify this hamiltonian. At first sight the Cu-O repulsion seems essential since a large charge-transfer is expected. However, V_{dp} is usually much smaller than the on-site repulsions and, furthermore, this term gives rise to new physics only in the event of exciton formation. Hence, if we are not especially interested in these processes, V_{dp} can be safely ignored. One is then left with a charge-transfer model Hamiltonian which can still give a reasonable description of some of these compounds^{12,13}, e.g., SrCuO_2 and Sr_2CuO_3 ⁷. If we are now willing to reduce the number of parameters by putting (somewhat arbitrarily) $U_{pp} = U_{dd}$, then the so-called ionic Hubbard model (IHM) follows. It can be written simply as

$$H = t \sum_{\langle ij \rangle s} c_{is}^{\dagger} c_{js} + \frac{U}{2} \sum_{is} (1 - \tau_i) n_{is} + U \sum_i n_{i\#} n_{i\#} \quad (2)$$

where τ_i is the on-site energy difference between even and odd sites, usually known as the charge-transfer energy.

Although, strictly speaking, this Hamiltonian does not describe accurately any specific system (since quite generally $U_{pp} < U_{dd}$), it provides a simple, minimal, model where the interplay among covalency (t), ionicity (τ_i) and correlation (U) gives rise to a rich phase diagram within which different 1D compounds can be placed. Originally proposed by Nagaosa and Takimoto¹⁴ as a model for ferroelectric perovskites and later by Egami et al^{15,16} to explain the neutral-ionic transition in some organic crystals, this Hamiltonian is ideal for studying the nature of quantum phase transitions in 1D electron systems. On general grounds, one expects a transition from an ionic, weakly-correlated band insulator (BI) phase to a neutral, strongly-correlated Mott insulator (MI) phase as U increases. An important and controverted issue is the nature of this transition as well as whether two critical points rather than one separate both phases. Depending on the method of calculation used, either one^{17,18,19} or two^{20,21,22,23} critical points have been predicted, so that the controversy cannot be considered as closed yet.

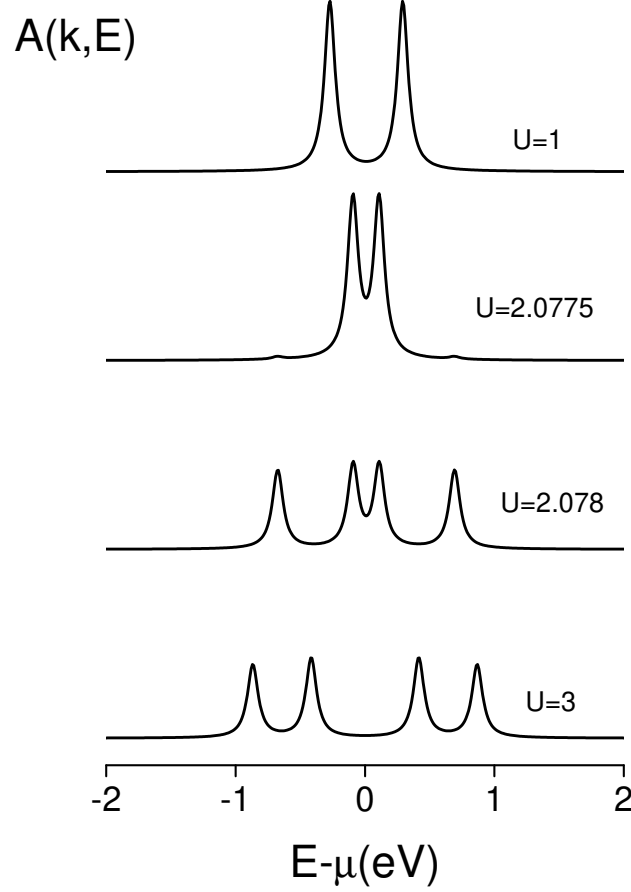


FIG. 1: Single-particle spectral-weight function $A(k; E)$ for the half-filled ionic Hubbard model at the Fermi points $k = \pm 2$. From top to bottom, $U = 1, 2.0775$ (just below U_c), 2.078 (just above U_c), and 3 . We have taken $t = 1$ and $v = 1$. All the energies are given in eV.

In this paper we stay outside this controversy and will rather concentrate on the single-particle spectral-weight function (SWF) $A(k; !)$ of the 1D IHM at half filling, which can be compared with ARPES of several insulating materials. $A(k; !)$ will be calculated using the cluster perturbation theory (CPT) approach of Senechal et al.²⁴. This is briefly described in Sec II. Sec III gives our results for $A(k; !)$ (a sudden change of regime at a critical value of U) followed by a discussion showing that $(\text{TaSe}_4)_2\text{I}$ and $\text{K}_{0.3}\text{MnO}_3$, are good examples of these two regimes. Finally, Sec IV closes the paper with some concluding remarks.

II. CLUSTER PERTURBATION THEORY (CPT)

Since this method has been discussed at length in Ref 24, we simply summarize it very briefly here. In CPT one divides the lattice (here the chain) into a number of equal clusters. The single-particle Green's function (GF) on these clusters is then found by exact diagonalization with open boundary conditions. We have made use of a variant of the Lanczos algorithm specially designed to calculate dynamic quantities²⁵. The approximation now consists in neglecting the intercluster selfenergy, so that the GF's of neighboring clusters are connected by hopping terms only. Periodic boundary conditions are then imposed on the whole chain, i.e., between the extreme clusters. To be specific, let m denote the site m of the cluster i . The exact Greens function G_{mij} , of the whole chain is given by the well-known Dyson's equation in matrix form $(G_0^{-1} - \Sigma)G = I$, in terms of the non-interacting GF and the exact Σ . In CPT this exact Σ is approximated by $\Sigma_{mij} = \delta_{ij} \Sigma_{mn}^C$ where Σ^C is the cluster self-energy matrix. This approximation is applicable to any lattice in any dimension. It can be understood as a lowest-order contribution to a systematic perturbation expansion in powers of the intercluster hopping^{24,26}. It turns out, on the other hand, that CPT is a limiting case of a more general variational cluster approach²⁷.

In this paper we concentrate on the SW F A ($k; !$), given as usual by

$$A(k; !) = \frac{1}{-i\pi} \text{Im} G(k; ! + i) \quad (3)$$

where $G(k; !)$ is the Fourier transform (FT) of the single-particle retarded GF and $!$ a small positive number. This FT must be calculated with some care since $G_{mn}(i - j)$ is periodic in ij but not in mn due to the open boundary conditions used in the clusters. The correct formula is^{24,26}

$$G(k; !) = \frac{1}{N} \sum_{mn} e^{ik(m-n)} G_{mn}(N k; !) \quad (4)$$

where N is the number of sites in a cluster and $G_{mn}(k)$ the FT of $G_{mn}(i - j)$.

III. THE SPECTRAL WEIGHT FUNCTION OF THE IONIC HUBBARD MODEL AT HALF FILLING

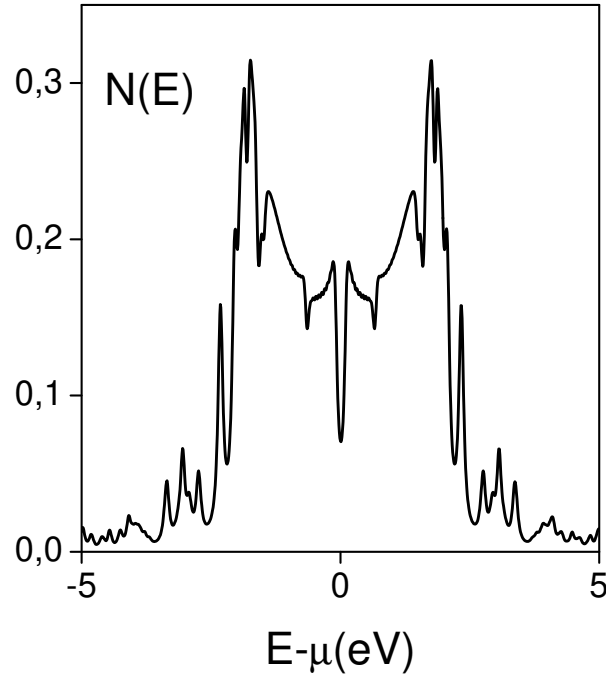


FIG. 2: Density of states for the same model of Fig 1 with $U = 2.0775$, eV just below U_c .

We consider a chain of ninety-six sites of two kinds with levels at $\epsilon = 2$, at half filling, and take $t = 1$ eV and $\epsilon = 1$ eV. Clusters of eight sites have been adopted after checking that increasing the cluster size up to twelve sites does not change much the results for the whole chain. Fig 1 shows $A(k; E)$ at the Fermi points $k_F = \pm 2$ for increasing U . A broadening $\gamma = 0.05$ eV has been given to the otherwise delta functions. Two regimes are observed in the low-energy region: For small U , a two-peak structure is seen close to the chemical potential (zero reference-energy). This structure persists, while the two peaks approach each other, up to $U = 2.0775$ eV. Abruptly, at $U = U_c = 2.078$ eV a four-peak structure appears, with the peak heights being roughly half those of the previous two-peak structure. It seems, therefore, that each of the latter peaks splits, developing a new peak at higher energy and thus leading to the new four-peak structure. As U further increases, the inner peaks, closer to the chemical potential, start to separate from each other quickly approaching the outer peaks which in turn move apart more slowly. Finally, for very large U , much larger than t and ϵ , the SWF tends asymptotically to a Mott-Hubbard situation without any signature of abrupt change. The single-particle (charge) gap, after passing through a minimum at U_c , increases again. It never vanishes, in agreement with recent

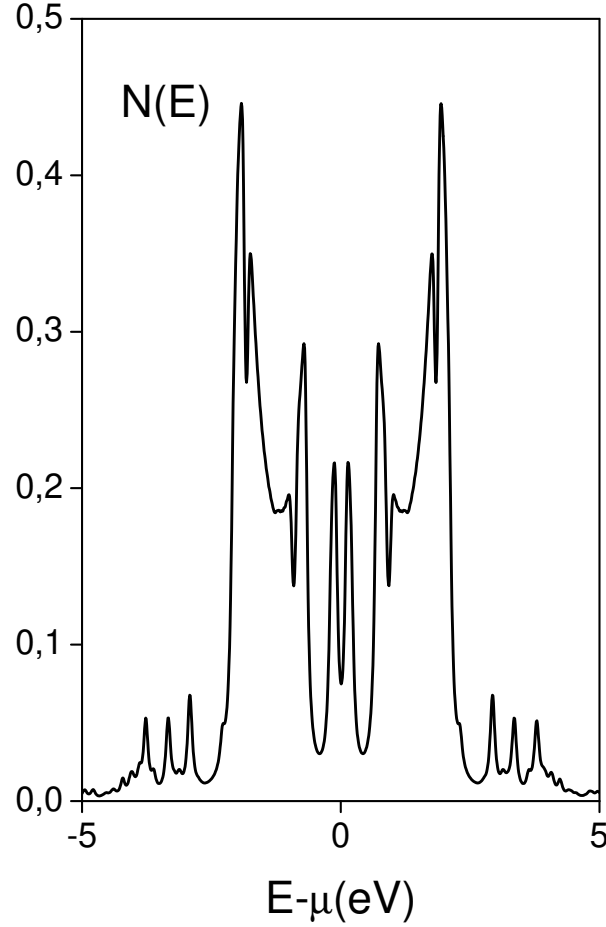


FIG. 3: The same as Fig 2 but for $U = 2.0780$, eV just above U_c

ndings^{19,23}.

A somewhat different, but complementary perspective is afforded by the density of states (DOS), $N(E) = \frac{1}{M} \sum_k A(k; E)$, where M is the number of k 's. Fig 2 shows the DOS for $U = 2.0775$ eV, just below U_c . It is reminiscent of the non-interacting DOS (a branch-cut surrounded by two singularities and cut by a gap at the chemical potential). This region $U < U_c$, is the band insulating regime, the DOS being similar to that for $U = 0$, but with a continuously decreasing gap. Fig 3, on the other hand, displays the DOS for $U = 2.078$ eV, just above U_c , in correspondence with the third panel (from top to bottom) of Fig 1. The two outer peaks in this latter figure mark the top (bottom) of the occupied (empty) Hubbard band. The two inner peaks stand isolated near the chemical potential resembling two "impurity-like", non-dispersive peaks within the (wider) gap between the Hubbard bands. All through the region $U > U_c$, the DOS is quite different from that at

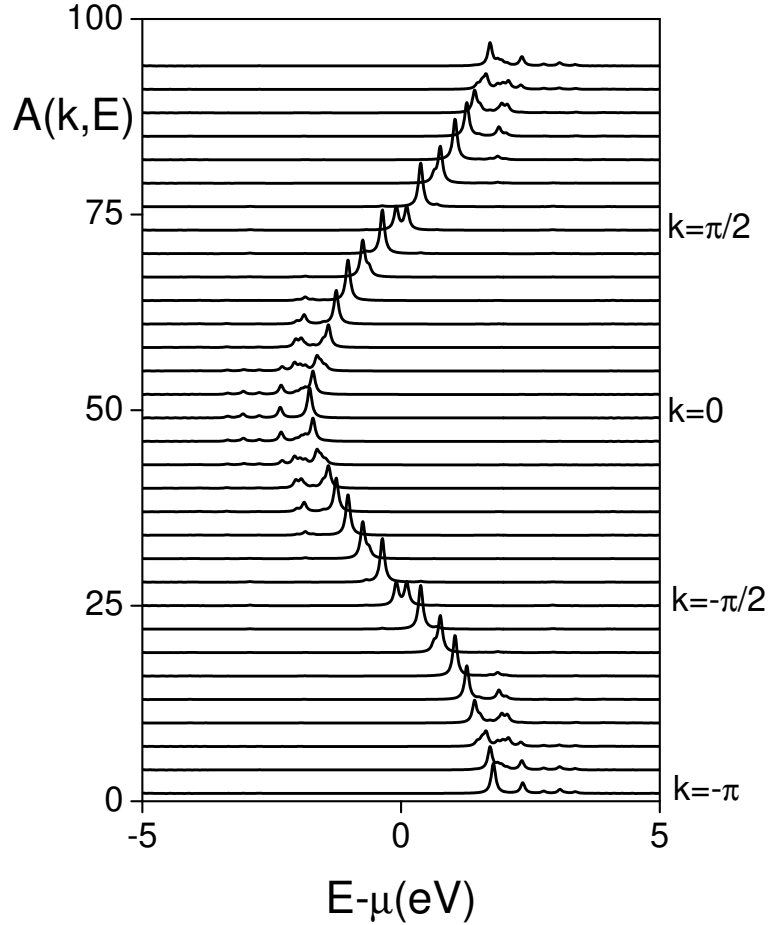


FIG. 4: Spectral weight function $A(k; E)$ for the same situation of Fig 2. An offset has been given to the plots for different k 's along the large Brillouin zone ($k < \pi$) in order to avoid superposition. The figures along the left vertical axis count the number of k 's starting from 0. On the right vertical axis, some special k 's are indicated

$U = 0$.

To check what changes have taken place at $k \neq \pi/2$, Figs 4 and 5 display $A(k, E)$ for the same U values as the above DOS along the large Brillouin Zone (BZ), $k < \pi$ (in the extended zone scheme). The portion $k \geq \pi/2$ can be mapped, if one wishes, onto the small BZ giving the empty bands for $k \geq \pi/2$ above the occupied bands. An offset has been provided to the different plots to avoid superposition. The figures along the vertical axis number the k 's starting from $k = 0$ (only a selected set of thirty-two k 's have been shown for clarity). Fig 4 shows a cosine-like band cut in two by a gap at the Fermi points (cfr. with the second panel in Fig 1). Two shadow bands covering only part of the BZ are clearly

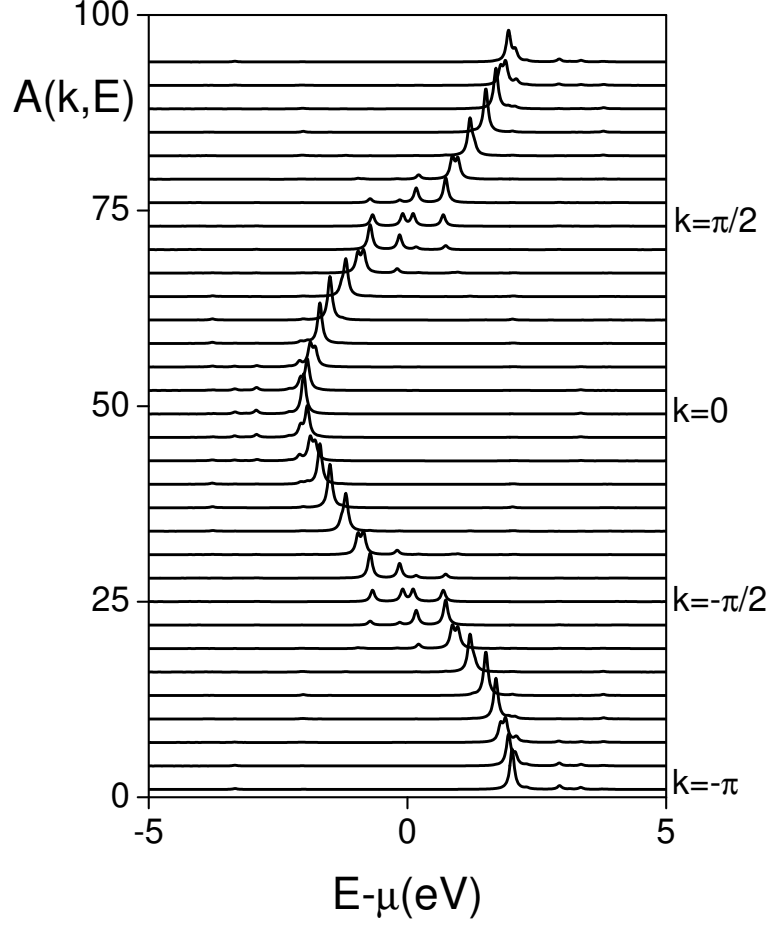


FIG. 5: Same as Fig 4, but for $U = 2.0780$, eV just above U_c

visible around $k = 0$ (occupied) and $k = \pi$ (empty). They give rise to the side-peaks to the left and right of the main body of the DOS of Fig 2. Fig 5 should now be confronted with the DOS of Fig 3. The cosine-like band is now cut by a wider gap delimited by the outer peaks of Fig 1, third panel. The inner peaks are continued by two almost non-dispersive, flat bands covering only a small portion of the BZ around k_F are clearly visible. The shadow bands around $k = 0$ and $k = \pi$ have now almost disappeared along with the side-peaks, rather weak in Fig 3.

It is difficult to extract the character of the peaks in a calculation based on a Lanczos algorithm, and much more so to trace the origin of the change of regime just described. However, these regimes must have some physical reality since we observe that both are found in ARPES of different Q1D insulating materials. Since most of these materials have occupied bands with roughly 1eV of bandwidth, we have accordingly taken $t = 0.5$ eV and

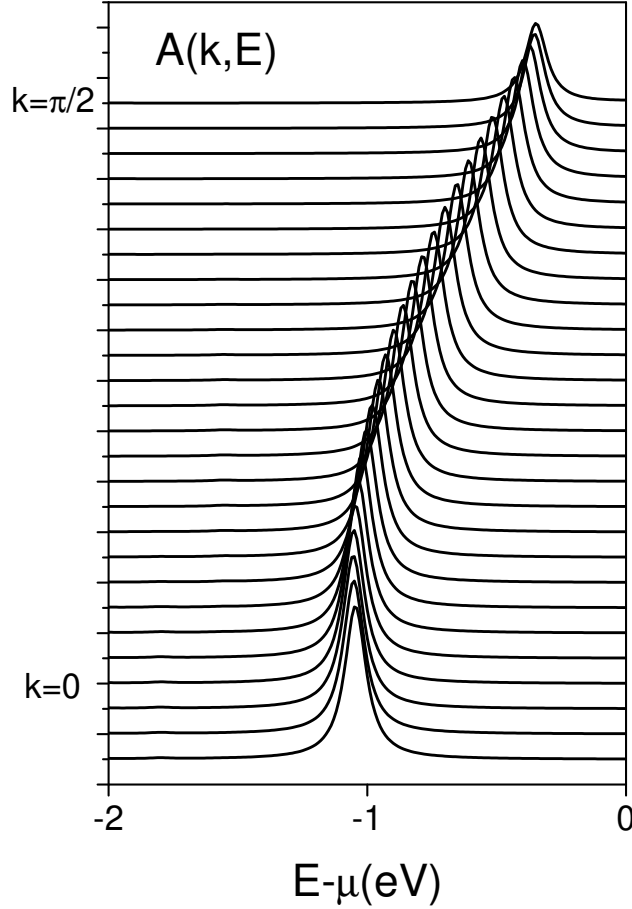


FIG . 6: Spectral-weight function for (in eV) $t = 0.5$, $\mu = 1$ and $U = 0.5$

$\mu = 1\text{eV}$. The critical U separating both regimes is now $U_c = 2\text{eV}$. Let us take, just for illustrative purpose, $(\text{TaSe}_4)_2\text{I}$, and $\text{K}_{0.3}\text{MnO}_3$, Fig 6 shows $A(k; E)$ between $k = 0$ and $\pi/2$ for $U = 0.5\text{eV} < U_c$, a case of the first regime, with a single occupied peak at $k = \pi/2$. This one-band structure resembles that of $(\text{TaSe}_4)_2\text{I}$ in the direction parallel to the chain (compare with Fig 2a of Ref 3). Likewise, Fig 7 shows the same information as Fig 6, but for $U = 2.1\text{eV} > U_c$. We now see a two-band structure in the neighborhood of $k = \pi/2$. This resembles the band structure of $\text{K}_{0.3}\text{MnO}_3$ (compare with Fig 15 of Ref 4).

IV . CONCLUSIONS

Using the cluster perturbation theory approach of Senechal et al^{24,26}, we have calculated the single-particle spectral-weight function $A(k; E)$ of the ionic 1D Hubbard model at half filling. A change of regime is found at a critical value of U , $U_c(t; \mu)$, which depends on

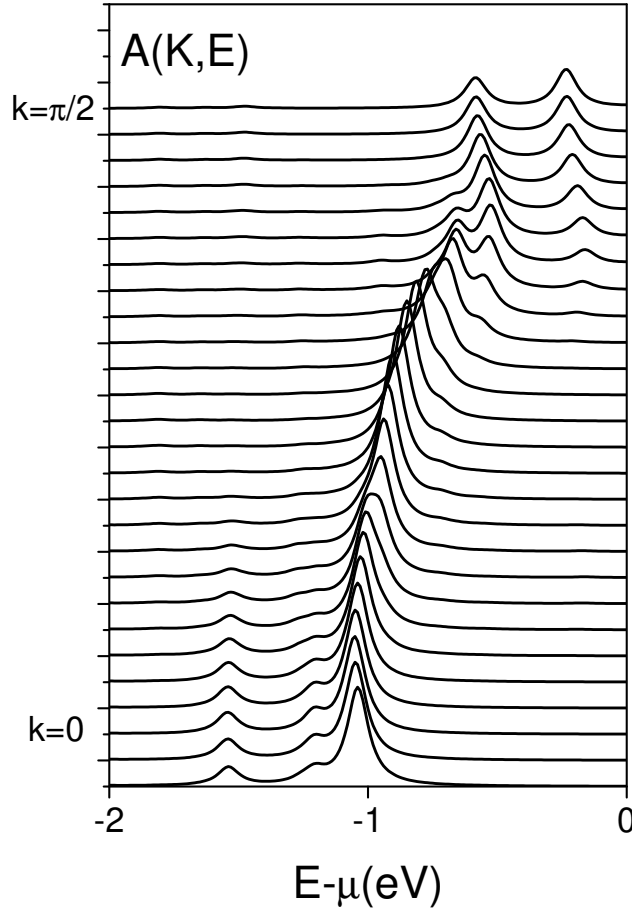


FIG. 7: The same as Fig 6, but for $U = 2.1$ eV

both the hopping amplitude t and the on-site energy difference, ϵ , between even and odd sites. As U increases, $A(k; \omega)$ jumps from a two-peak structure to a four-peak one at the Fermi points $k_F = \pm 2$. As one moves away from k_F , one finds two semiconducting bands, for $U < U_c$, separated by a gap which decreases from its initial value (at $U = 0$) down to a small, but non-vanishing, value at U_c . This gap is always delimited by the two-peak structure at k_F . For $U > U_c$, instead, two at, almost non-dispersive bands appear around the Fermi points as the continuation of the inner peaks in the four-peak structure. They fade away very soon. The gap between them now increases from its minimum value at U_c . The outer peaks mark the top (bottom) of the lower (upper) Hubbard-like bands. As U increases further, the at bands approach the Hubbard bands, finally merging into them. Asymptotically, a Mott-Hubbard situation is approached in a continuous way, without any signature of abrupt change in $A(k; \omega)$ in this region of large U .

Alternatively we can say that, for $U < U_c$, the two-band structure is continuously connected to the band insulator shape at $U = 0$. This is the band insulator regime. For $U > U_c$, two new flat bands appear and push the two wider bands of the first regime further apart. This is the second regime, more Hubbard-like, which goes to the Mott-Hubbard regime at large U . Different Q1D materials have band structures which can be classified as lying in either the first or the second regime.

We acknowledge the financial support of the Spanish DGICYT through Project BFM 2002-01594

Electronic address: refolio@inam.cfm.ac.csic.es

- ¹ F D M Haldane J. Phys. C 14,2585 (1981)
- ² Y Hwu, P Almaras, M Marsi, H Berger, F Levy, M G rioni, D M alterre, and G M argaritondo Phys. Rev.B 46,13624 (1992)
- ³ A Terrasi, M Marsi, H Berger, G M argaritondo, R J K elley, and M . O nellion. Phys. Rev.B 52,5592 (1995)
- ⁴ G H G weon, J D Denlinger, J W Allen, R C laesson, C G O lson, H H ochet, J M arcus, C Schlenker, and L F Schneem eyer J Electron Spectrosc. Rel. Phen. 117-118, 481 (2001)
- ⁵ F Z wick, D J erome, G M argaritondo, M O nellion, J Vo it, and M G rioni Phys.Rev.Lett. 81, 2974 (1998)
- ⁶ M Sing, U Schwingenschlo gl, R C laesson, P B laha, J M P C arm elo, L M M arteb, P D Sacram ento, M D ressel, and C S Jacobsen Phy.Rev.B . 68,125111 (2003)
- ⁷ M G rioni, and J Vo it Electron Spectroscopies Applied to Low-D im ensional M aterials, edited by H Starnberg and H Hughes (K l uwer, D ordrecht 2000 Vol 1.)
- ⁸ K Penc, and W Stephan Phy.Rev.B . 62,12707 (2000)
- ⁹ C K im , A Y Matsuura, Z-X Shen, N M otoyam a, H E isaki, S J chida, T Tohyam a, and S M aekawa Phy.Rev.Lett. 77,4054 (1996)
- ¹⁰ R Neudert, M K nupfer, M S G olden, J F ink, W Stephan, K Penc, N M otoyam a, H E isaki, and S J chida Phy.Rev.Lett. 81,657 (1998)
- ¹¹ V J Em ery Phy.Rev.Lett. 58,2794 (1987)

- ¹² J.Zanen, G A Sawatzky, and J W Allen Phys. Rev.Lett 55,418 (1985)
- ¹³ M B Meinders, H Eskes, and G A Sawatzky Phy.Rev.B . 48,3916 (1993)
- ¹⁴ N Nagaosa, and J.Takimoto J. Phys. Soc.Jpn 55,2735 (1986)
- ¹⁵ T Egami, S.Ishihara, and M Tachiki Science 261,1307 (1993)
- ¹⁶ S.Ishihara, T Egami, and M Tachiki Phy.Rev.B . 49,8944 (1994)
- ¹⁷ R Resta, and S.Sorella Phys. Rev. Lett 74, 4738 (1995)
- ¹⁸ T Wilkens, and R Martin Phys. Rev. B 64, 235108 (2001)
- ¹⁹ A P Kampf, M .Sekanina, G .I.Japaridze, and Ph Brune J.Phys. Condens. Matter 15, 5895 (2003)
- ²⁰ M Fabrizio, A Gogolin, and A A Nersisyan Phys. Rev. Lett 83, 2014 (1999)
- ²¹ Y Takada, and M Kido J. Phys. Soc. Jpn 70, 21 (2001)
- ²² Y Z Zhang, C O Wu, and H Q Lin Phys. Rev. B 67, 205109 (2003)
- ²³ S.R Manmana, V M eden, R M Noack, and K Schonhammer cond-mat/0307741
- ²⁴ D Senechal, D Perez, and M Pioro-Ladriere Phys. Rev. Lett 84, 522 (2000)
- ²⁵ E Dagotto Rev. Mod. Phys 66, 763 (1994)
- ²⁶ D Senechal, D Perez, and D Pabue Phys. Rev. B 66, 075129 (2002)
- ²⁷ M Potthof, M Aichhorn, and C Dahnen Phys. Rev. Lett 91, 206 (2003)